Carbon Letters (2019) 29:319–326
https://doi.org/10.1007/s42823-019-00046-8

Online ISSN 2233-4998
Print ISSN 1976-4251

NOTES

Kinetics and dynamic adsorption of methylene blue by CO_2-activated resorcinol formaldehyde carbon gels

Azrul Nurfaiz Mohd Faizal[1,2] · Muhamad Hazim Abdul Halim[2] · Muhammad Abbas Ahmad Zaini[1,2]

Received: 30 October 2018 / Accepted: 18 February 2019 / Published online: 25 May 2019

Abstract
The present work is aimed at evaluating the kinetics and dynamic adsorption of methylene blue by CO_2-activated carbon gels. The carbon gels were characterized by textural properties, thermal degradation and surface chemistry. The result shows that the carbon gels are highly microporous with surface area of 514 m^2/g and 745 m^2/g for resorcinol-to-catalyst ratios of 1000 (AC1) and 2000 (AC2), respectively. The kinetics data could be described by pseudo-first-order model, with a longer duration to attain equilibrium due to restricted pore diffusion as concentration increases. Also, AC1 exhibits insignificant kinetics with fluctuating adsorption with time at concentrations of 20 and 25 mg/L. However, AC1 reveals a better performance than AC2 in dynamic adsorption due to concentration gradient for molecules diffusion to active sites. The applicability of Yoon–Nelson and Thomas models indicates that the dynamic adsorption is controlled by external and internal diffusion.

Keywords Adsorption · Carbon gel · CO_2 activation · Methylene blue

1 Introduction

There is a burgeoning concern over the presence of contaminants in water bodies from various industrial sectors. The effluent bearing carcinogenic and toxic substances such as heavy metals, organic compounds and dyes is harmful to aquatic ecosystem, public health and food chains. The presence of dyes in water prevents the penetration of sunlight, hence affecting the photosynthesis of aquatic plants. Consequently, the scarce of oxygen in water for respiration may result in the death of aquatic creatures [1]. Methylene blue is an example of the commonly used dye in fabric and textile factories. It is hazardous and can cause profuse sweating, nausea and mental confusion [2]. Similar to the other types of water contaminants, the removal is essential to maintain a pollution-free environment for the well-being of ecosystem.

In general, the wastewater treatment strategies can be categorized as physical, chemical and biological methods, or combination of any of these methods. Among others, adsorption onto microporous and mesoporous materials is a preferable technique to treat dyes-containing wastewater because it is cheap, simple, effective and easy to operate and scale-up [3]. Activated carbon adsorption has proven to yield a high removal capacity of water pollutants even at trace concentrations through various mechanisms such as pore-filling, π–π interaction, ion exchange and formation of chelate/complex [4]. In real industrial process that deals with a large volume of wastewater, adsorption through continuous mode is more preferable because of minimum manufacturing costs and less space needed. However, the column operation is prone to escalating pressure drop due to hydraulic resistance. Consequently, this may result in high operating costs and poor column performance.

Carbon gel is a promising porous carbon with a highly flexible shape, pore texture and nanostructure. It is produced through polymerization of resorcinol and formaldehyde in the presence of solvent (water) and basic catalyst (sodium carbonate) and can be moulded into a particular shape to elicit the desired type of column packing, from which the surface contact can be maximized, and the hydraulic pressure inside the column can be reduced [5]. The density of mesopores and micropores of carbon

✉ Muhammad Abbas Ahmad Zaini
abbas@cheme.utm.my

[1] Centre of Lipids Engineering and Applied Research, Ibnu-Sina Institute for Scientific and Industrial Research, Universiti Teknologi Malaysia, 81310 UTM Johor Bahru, Johor, Malaysia

[2] School of Chemical and Energy Engineering, Faculty of Engineering, Universiti Teknologi Malaysia, 81310 UTM Johor Bahru, Johor, Malaysia

gel can be tailored independently by adjusting the process conditions to control the voids formed during the aggregation of nanoparticles [6, 7]. Recently, our group has reported some dyes removal by carbon gels in batch mode [8–10]. The removal performance has been established and was found to be comparable with other adsorbents in the literature. To date, however, the use of carbon gel in column adsorption is not widely explored in much of the published literature. To unlock its true potential, therefore, the present work is aimed to evaluate the kinetics and column parameters of methylene blue by CO_2-activated carbon gels. Several models were employed to discuss the removal mechanisms.

2 Materials and methods

2.1 Materials

Resorcinol ($C_6H_6O_2$, mw = 110.11 g/mol, assay 99%), formaldehyde (HCHO, mw = 30.03 g/mol, 37 w/w % in water), sodium carbonate (Na_2CO_3, mw = 105.99 g/mol, assay 99.5%), tert-butyl alcohol ($(CH_3)_3COH$, mw = 74.12 g/mol, assay 99%) and methylene blue ($C_{16}H_{18}ClN_3S$, mw = 319.85 g/mol, assay 99%) were purchased from R&M Chemicals. Carbon dioxide was supplied by Mega Mount Gases. All chemicals are of analytical reagent grade.

2.2 Preparation and characterization of carbon gels

Resorcinol (25 g) and sodium carbonate (catalyst, 0.0241 g) were dissolved in a 29.73-g water. Next, a 36.85 g of formaldehyde was added into the solution. The resultant mixture (resorcinol/catalyst = 1000 mol/mol, designated as AC1) was stirred and poured into a mould and allowed at 35 °C for two days for gelation. Then, it was heated at 60 °C for three days for gel ageing. The solid gel was subjected to solvent exchange using tert-butyl alcohol at 50 °C for three days to remove excess water from the interior matrix. The solvent was replaced with the fresh one twice a day. After that, the dried gel was ground to a size of 0.5 cm. Finally, it was activated in a tubular furnace at 900 °C for 1 h under CO_2 flow. The steps were repeated for a different catalyst amount (resorcinol/catalyst = 2000 mol/mol, designated as AC2).

The carbon gels were characterized for textural properties using a surface area analyzer (Pulse Chemisorb 2705, Micrometrics). The surface functional groups of carbon gels were determined using a FTIR spectrometer (Spectrum One, PerkinElmer). The thermogravimetric analysis was performed under N_2 flow using a TGA analyzer (PerkinElmer).

2.3 Adsorption studies

2.3.1 Adsorption kinetics

A fixed carbon gel weight of 0.05 g was added into a flask containing 50 mL of methylene blue solution of specified concentrations of 5 mg/L, 10 mg/L, 20 mg/L and 25 mg/L. The residual concentration was measured at different time intervals for 480 h. The adsorption capacity at time t was computed as $q_t = (C_0 - C_t)V/m$, where q_t (mg/g) is the adsorption capacity at time t, C_0 (mg/L) is the initial concentration, and C_t (mg/L) is the concentration measured at time t. The residual concentration was measured using a UV–Vis spectrophotometer (DU 8200, Drawell Scientific) at a wavelength of 620 nm.

2.3.2 Column adsorption

A fixed carbon gel weight of 1 g was loaded in a column (internal diameter = 0.7 cm, height = 7.75 cm) which forms a bed through which the methylene blue solution is passed and continuously meets a fresh part of the solid gel and tends to establish a new equilibrium. A peristaltic pump was used to pump the liquid into the column from the bottom and leaving the column top. The feed flow rates and concentrations were varied at 0.5 mL/min and 1 mL/min, and 2 mg/L and 10 mg/L, respectively, and the effluent concentration was measured at preset time intervals until $C_t/C_0 = 1$.

The adsorption data were analyzed using kinetics and column models. Table 1 summarizes the kinetics constants, column models and column parameters.

3 Results and discussion

3.1 Characteristics of carbon gels

Table 2 shows the yield and textural characteristics of AC1 and AC2. A high catalyst content in the preparation of carbon gel often results in a polymeric gel of small particles in a well-connected configuration, while a colloidal gel of spherical particles connected by narrow necks could be produced under a low catalyst content [16]. From Table 2, an increase in resorcinol-to-catalyst ratio contributes to a higher pore volume and surface area [17, 18]. Upon CO_2 treatment at 900 °C, AC2 exhibits a specific surface area of 745 m^2/g that is higher than AC1 (514 m^2/g). The configuration of particles agglomeration in AC2 gives rise to more voids that brings about rich textural characteristics. Yet, this may as well result in a lower yield due to the collapse of narrow neck structure that triggers excessive burning off and

Table 1 Kinetics models, column models and column parameters

Kinetics model			
Pseudo-first-order [11]			
$q_t = q_e\left[1 - e^{-k_1 t}\right]$	q_t (mg/g)	:	Adsorption at time, t
	k_1 (h^{-1})	:	Pseudo-first-order adsorption rate constant
	t (h)	:	Contact time
Pseudo-second-order [12]			
$q_t = \frac{k_2 q_e^2 t}{\left(1 + k_2 q_e t\right)}$	k_2 (g/mg h)	:	Pseudo-second-order adsorption rate constant
$h = k_2 q_e^2$			
	h (mg/g h)	:	Initial adsorption rate
Column model			
Yoon–Nelson [13]			
$\ln\left(\frac{C_t}{C_0 - C_t}\right) = K_{YN}t - \tau K_{YN}$	K_{YN} (min^{-1})	:	Yoon–Nelson rate constant
	τ (min)	:	Time needed for 50% breakthrough
Adams–Bohart [14]			
$\ln \frac{C_t}{C_0} = K_{AB}C_0 t - K_{AB}N_0\frac{Z}{U_0}$	K_{AB} (L/mg.min)	:	Adams–Bohart rate constant
	N_o (mg/L)	:	Saturation concentration
	Z (cm)	:	Bed height
	U_o (cm/min)	:	Superficial velocity
Thomas [15]			
$\ln\left(\frac{C_0}{C_t} - 1\right) = \frac{K_T q_T}{Q} - K_T C_0 t$	K_T (L/mg.min)	:	Thomas rate constant
	q_T (mg)	:	Column capacity
	Q (L/min)	:	Volumetric flow rate
Column parameters			
Column capacity			
$q_{Total} = QA = Q\int\left(C_0 - C_t\right)dt$	A (mg.min/L)	:	Area under the curve
	Q (L/min)	:	Volumetric flow rate
Amount of solute supplied			
$W_{Total} = C_0 Qt$	t (min)	:	Column retention time

Table 2 Yield and textural characteristics of carbon gels

	AC1	AC2
Yield (%)	53.3	35.6
BET surface area (m^2/g)	514	745
Micropores area (m^2/g)	488	699
Mesopores area (m^2/g)	25.7	46.6
Micropores volume (cm^3/g)	0.18	0.26
Mesopores volume (cm^3/g)	0.0096	0.0207
Total pore volume of pores (cm^3/g)	0.193	0.283
Mesopore content (%)	4.97	7.31
Average pore diameter (nm)	1.50	1.52

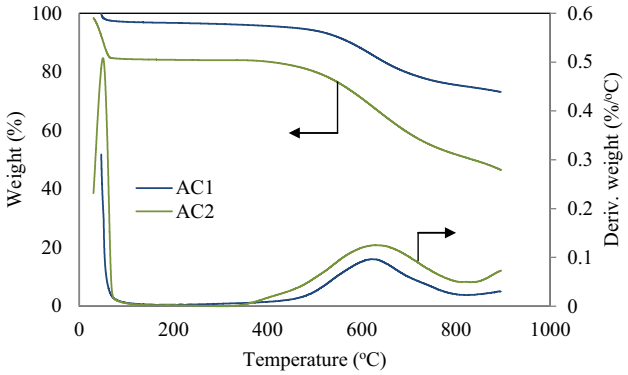

Fig. 1 Thermal degradation profiles of carbon gels

liberation of volatiles during carbonization. Both carbon gels are highly microporous (> 92% micropore content) with pore width about 1.50 nm. In the earlier works, Lin-Zhi and Zaini [9] and Zaini et al. [10] reported the mesoporous nature (> 60% mesopore content) of carbon gels via carbonization in a confined area at 600 °C and N_2 at 1000 °C, respectively. In this work, the use of CO_2 in carbonization could minimize the collapse of voids into mesopores.

Figure 1 shows the thermal decomposition profiles of carbon gels. The first peak at 50 °C corresponds to the loss of physisorbed moisture. At this temperature, AC2 displays a

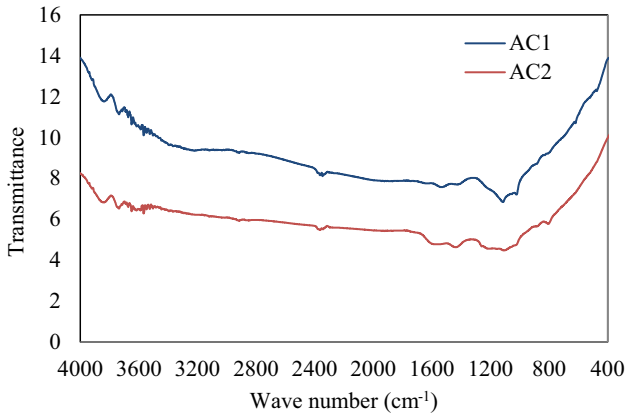

Fig. 2 FTIR spectra of AC1 and AC2

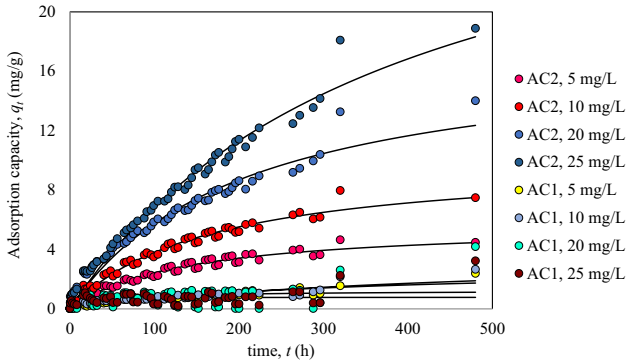

Fig. 3 Rate of methylene blue adsorption by carbon gels (Lines were predicted using pseudo-second-order model)

greater weight loss of 15%, attributed to its high pore volume to entrap moisture. Both carbon gels demonstrate a thermally stable character with trivial weight loss between 100 and 400 °C. AC1 and AC2 start to decompose at 520 °C and 493 °C, respectively. The second peak at 600 °C is associated with the liberation of carbon atoms from the materials. A greater weight loss of AC2, relative to that of AC1 at 900 °C could be related to its narrow neck configuration that is susceptible to collapse, at which the values of residual weight are 46.5% and 73.2%, respectively.

The FTIR spectra of AC1 and AC2 are shown in Fig. 2. Both carbon gels exhibit similar peaks of spectra. The peak at 3500 cm^{-1} is attributed to O–H bond stretching belonged to tert-butyl alcohol and physisorbed moisture. The peak at 2950 cm^{-1} is the characteristic of sp^3 C–H stretch, while that at 1530 cm^{-1} corresponds to sp^3 C–H bend. The peak at 1100 cm^{-1} represents C–O bending. A distinct peak of AC1 at 879 cm^{-1} is associated with meta-disubstituted aromatic, while that of AC2 at 800 cm^{-1} is para-disubstituted aromatic. In general, the carbon gels display a comparable surface chemistry with a slight difference due to textural properties as a result of different catalyst ratio. Similar finding has also been reported elsewhere [10].

3.2 Adsorption kinetics

Figure 3 shows the rate of methylene blue adsorption at different concentrations by AC1 and AC2. In general, the adsorption rate is high when dye molecules are initially in contact with adsorbent to a period when the rate starts to subside and the capacity becomes constant at equilibrium. At equilibrium, the rate of adsorption is equal to the rate of desorption.AC2 shows an increasing pattern of removal capacity with increasing concentration. A higher concentration offers a greater driving force to overcome solid mass transfer resistance for adsorption. In addition, a longer contact time is needed for AC2 to attain the state of equilibrium at a higher dye concentration. For comparison, Zaini and co-workers [10] reported a less duration of 50 h to attain equilibrium by mesoporous carbon gel as opposed to 480 h by microporous AC2 for the removal of 10 mg/L methylene blue. Nevertheless, AC2 demonstrates a slightly better equilibrium capacity of 7.5 mg/g, than the mesoporous carbon gel (4.4 mg/g) [10]. On the other hand, AC1 exhibits an inferior adsorption kinetics probably due to its lower surface area and mesopore volume than AC2. AC1 displays a fluctuating pattern of adsorption with time at values ranging between 0 mg/g and 3 mg/g, and it is more prevalent at concentrations of 20 mg/L and 25 mg/L, whereby several loops of adsorption and desorption were recorded. This could be due to continual lateral repulsion among dye molecules leading to desorption, hence leaving the sites vacant. This is supported by the fact that the dye molecules may lodge on the exterior of the pores due to the molecular size (1.1 nm) that is as fit as the pore (1.5 nm).

Table 3 summarizes the pseudo-kinetics constants of methylene blue adsorption at different concentrations by AC1 and AC2. AC2 shows a best fit to pseudo-first-order model with regression coefficient (R^2) close to unity, small sum of squared errors (SSE) and comparable q_e values with the experimental ones. Hence, the model is suitable to describe the rate of methylene blue adsorption by AC2 at concentrations studied. It implies that the external diffusion is a significant step in adsorption, and that the process is pore-filling or physical adsorption [11]. In addition, dye molecules may form imaginary bonds as a result of the mutual interactions with active sites on carbon gel via electrostatic interaction, and van der Waals and dispersive forces [19]. It is also suggested that the bonds are relatively weak, and the adsorption is therefore reversible.

From Table 3, the pseudo-second-order rate constant, k_2 of AC2 displays a decreasing trend with increasing concentration. A high rate constant is due to a weak activation energy as a result of less repulsion of molecules at low

Table 3 Pseudo-kinetics constants of methylene blue adsorption onto carbon gels

	5 mg/L		10 mg/L		20 mg/L		25 mg/L	
	AC1	AC2	AC1	AC2	AC1	AC2	AC1	AC2
$q_{e,\,exp}$ (mg/g)	2.37	4.46	2.64	7.47	4.17	14.0	3.22	18.9
Pseudo-first-order model								
q_e (mg/g)	2.09	4.26	3.22	7.35	0.87	12.95	0.73	21.85
k_1 (h^{-1})	0.003	0.008	0.002	0.007	0.05	0.006	0.21	0.004
SSE	1.65	3.21	3.61	5.96	25.0	29.8	12.7	26.3
R^2	0.857	0.964	0.739	0.975	0.109	0.961	0.063	0.981
Pseudo-second-order model								
q_e (mg/g)	2.85	5.70	3.78	10.1	1.21	17.7	0.76	32.86
k_2 (g/mg h)	0.001	0.001	0.0005	0.0006	0.02	0.0003	0.41	7.98×10^{-5}
h (mg/g h)	0.009	0.042	0.0078	0.061	0.03	0.090	0.24	0.086
SSE	1.53	2.73	3.52	4.77	24.4	23.3	12.5	23.2
R^2	0.860	0.967	0.717	0.979	0.136	0.966	0.070	0.982

concentration. However, it decreases as a result of intensified collision of molecules at high concentration. Similarly, a higher initial adsorption rate, h at a higher concentration is likely due to a stronger driving force to overcome mass transfer resistance for the removal of dye molecules. On the other hand, AC1 exhibits a lack of fit to both pseudo-kinetics models due to inconsistent adsorption profiles, except for concentrations of 5 mg/L and 10 mg/L. In an earlier work, Zaini and co-workers [10] reported a rate constant of 0.088 h^{-1} for 10 mg/L of methylene blue by N_2-treated mesoporous carbon gel (resorcinol-to-catalyst ratio of 1000). The value recorded by its counterpart in this work is comparatively small at 0.002 h^{-1} probably due to inherent microporosity that restricts the diffusion of dye molecules to pore channels.

3.3 Column adsorption

Figure 4 displays the breakthrough curves of methylene blue adsorption by carbon gels. The breakthrough curves demonstrate a sharp front followed by a broaden tail, signifying a favourable dynamic adsorption. The behaviour could be explained by solid mass transfer resistance that dominates the overall adsorption rate. The C_t/C_o gradually increases with time to a point of $C_t/C_o = 1.0$, at which the column is completely exhausted. The breakthrough time t_b was determined at $C_t/C_o = 0.1$. From Fig. 4, only AC1 ($C_o = 2$ mg/L, flow rate of 0.5 mL/min) exhibits a breakthrough time of 75 min. It also indicates a higher volume of dye solution that could be treated. A missing breakthrough for the other operating conditions could be due to poor retention of dye molecules on the surface, rendering a high C_t even at $t = 0$ min. Also, a lower flow rate results in a longer contact time as well as a shallow adsorption zone for a higher removal capacity. At a higher flow rate, the front of adsorption zone quickly reaches the column top, implying a fast exhaustion

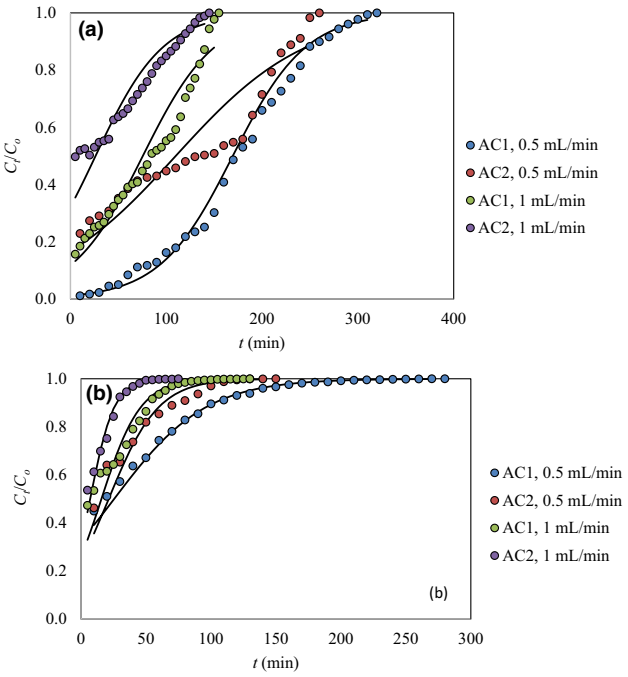

Fig. 4 Breakthrough curves of methylene blue adsorption by carbon gels at concentrations of (**a**) 2 mg/L and **b** 10 mg/L (Lines were predicted by Thomas model)

time of bed saturation. Similar pattern of breakthrough curve has been reported elsewhere [20, 21].

Table 4 summarizes the column parameters of methylene blue adsorption by AC1 and AC2 at different concentrations and flow rates. In general, the removal performance decreases with increasing flow rate and concentration. A higher flow rate caused a faster surface exhaustion due to insufficient residence time for dye molecules to diffuse into the pores. In dynamic adsorption, a higher concentration could result in repulsion among the molecules due

Table 4 Column parameters of methylene blue adsorption by carbon gels

	2 mg/L		10 mg/L	
	0.5 mL/min	1 mL/min	0.5 mL/min	1 mL/min
AC1				
Area under curve (mg min/L)	327	149	317	164
Retention time (min)	320	155	280	130
q_{Total} (mg)	0.164	0.149	0.159	0.164
W_{Total} (mg)	0.320	0.310		1.30
Per cent removal (%)	51.2	47.9	1.40	12.6
AC2				
Area under curve (mg.min/L)	224	72.9	188	76.3
Retention time (min)	260	145	150	75
q_{Total} (mg)	0.112	0.0729	0.0940	0.0763
W_{Total} (mg)	0.260	0.290	0.750	0.750
Per cent removal (%)	43.0	25.1	12.5	10.2

to increasing load to the surface. In either situations, the molecules are leaving the column before the equilibrium is attained, hence decreasing the removal capacity. From Table 4, interestingly, AC1 exhibits a greater removal performance than AC2. For example, at $C_o = 2$ mg/L (flow rate of 1 mL/min), AC1 shows a 47.9% removal as opposed to a 25.1% by AC2. Despite a lower surface area (mesoporosity), AC1 thrives in dynamic setting because of concentration gradient between the molecules and deficient active sites that provides a greater driving force and ample time for molecules diffusion in adsorption.

Table 5 summarizes the constants of column models. At $C_o = 10$ mg/L, the dynamic adsorption data are not fitted to Adams–Bohart model due to poor regression coefficient. However, the column behaviour could be satisfactorily described by Yoon–Nelson and Thomas models. Yoon and Nelson model is generally used to describe a decrease in adsorption rate that is proportional to the interaction probability between adsorption and adsorbent breakthrough [13]. From Table 5, the Yoon–Nelson rate constant K_{YN} increased with increasing flow rate and concentration, but the time required for 50% adsorbate breakthrough, τ, decreased. A high flow rate reduces the residence time, thus decreasing τ for an early saturation. AC2 displays a greater K_{YN} due to slow diffusion and rapid bed exhaustion. On the other hand, AC1 shows a greater τ, attributed to a higher methylene blue removal at the mass transfer zone because of a longer contact time. The first three values of τ in Table 5 are in agreement with half of retention time of reasonably ideal S-shaped breakthrough curves at $C_o = 2$ mg/L (Table 4 and Fig. 4). The agreement with Yoon–Nelson model implies that the adsorbent-phase mass transfer resistance is dominating the overall adsorption rate.

Adams–Bohart model [14] is mainly used to describe the initial part of breakthrough curve, wherein the rate of adsorption is proportional to the remaining capacity of adsorbent and adsorbate concentration. From Table 5, this model fitted well with the dynamic data at $C_o = 2$ mg/L. The rate constant K_{AB} decreased with increasing feed concentration, but increased with increasing flow rate, signifying that the dynamic behaviour is strongly influenced by external mass transfer [22]. Also, the saturation capacity N_o increased with increasing concentration.

Thomas model is used to explain a non-axial dispersion of plug flow behaviour based on adsorption that obeys Langmuir isotherm and second-order kinetics [15]. It satisfactorily describes the breakthrough behaviour of methylene blue adsorption onto CO_2-activated carbon gels, suggesting that the column operation is not controlled by external and internal diffusion [23]. Also, the values of column capacity q_T by this model agreed well with the experimental values as shown in Table 4.

4 Conclusion

The kinetics and dynamic adsorption of methylene blue were evaluated using microporous CO_2-activated carbon gels. A resorcinol-to-catalyst ratio 2000 (AC2) shows a higher specific surface area (745 m^2/g) than that of ratio 1000 (AC1). Accordingly, the performance of AC2 surpasses that of AC1 in adsorption kinetics, from which the behaviour could be described by pseudo-first-order model. Nevertheless, the equilibrium time is longer due to restricted pore diffusion as the concentration increases. In dynamic adsorption, AC1 reveals a better performance than AC2 due to concentration gradient that offers a greater driving force and ample time for molecules diffusion to active sites. The dynamic adsorption data obey Yoon–Nelson and Thomas models, suggesting that the external and internal diffusion steps are significant, especially at higher concentration.

Table 5 Constants of dynamic models

	C_0 (mg/L)	Flow rate (mL/min)	Yoon–Nelson				Adams–Bohart				Thomas			
			K_{YN} (min^{-1})	τ (min)	R^2	SSE	K_{AB} (L/mg.min)	N_0 (mg/L)	R^2	SSE	K_T (L/mg.min)	q_T (mg)	R^2	SSE
AC1	2	0.5	0.0262	169	0.975	4.29	6.78×10^{-3}	86.6	0.890	5.64	1.31×10^{-2}	0.170	0.975	4.29
AC2	2	0.5	0.0146	110	0.787	7.54	2.60×10^{-3}	88.3	0.961	0.14	7.31×10^{-3}	0.110	0.787	7.54
AC1	2	1.0	0.0266	75.5	0.864	6.30	5.66×10^{-3}	101	0.986	0.10	1.33×10^{-2}	0.151	0.864	6.30
AC2	2	1.0	0.0283	26.1	0.879	5.04	2.79×10^{-3}	89.4	0.985	0.02	1.42×10^{-2}	0.0524	0.879	5.04
AC1	10	0.5	0.0284	25.5	0.986	1.82	2.39×10^{-4}	345	0.704	0.39	2.85×10^{-3}	0.127	0.986	1.82
AC2	10	0.5	0.0523	21.3	0.933	4.45	4.81×10^{-4}	191	0.790	0.14	5.23×10^{-3}	0.107	0.933	4.45
AC1	10	1.0	0.0663	15.7	0.984	2.37	5.51×10^{-4}	325	0.788	0.27	6.64×10^{-3}	0.157	0.984	2.37
AC2	10	1.0	0.109	7.05	0.988	0.81	8.65×10^{-4}	185	0.766	0.13	1.09×10^{-2}	0.0705	0.988	0.81

Acknowledgements This work is supported by Ministry of Education, Malaysia, through Fundamental Research Grant Scheme (FRGS) No. 4F995.

References

1. Ming-Twang S, Zhi-Yong Q, Lin-Zhi L, Pei-Yee AY, Zaini MAA (2015) Dyes in water: characteristics, impacts to the environment and human health, and the removal strategies. In: Taylor JC (ed) Advances in chemistry research, vol 23. Nova Science Publishers Inc, New York, pp 143–156
2. Zaini MAA, Cher TY, Zakaria M, Kamaruddin MJ, Mohd-Setapar SH, Che-Yunus MA (2014) Palm oil mill effluent sludge ash as adsorbent for methylene blue dye removal. Desalin Water Treat 52(19–21):3654–3662
3. Shu-Hui T, Zaini MAA (2016) Dyes—classification and effective removal techniques. In: Taylor JC (ed) Advances in chemistry research, vol 30. Nova Science Publishers Inc, New York, pp 19–34
4. Ming-Twang S, Lin-Zhi L, Zaini MAA, Zhi-Yong Q, Pei-Yee AY (2015) Activated carbon for dyes adsorption in aqueous solution. In: Daniels JA (ed) Advances in environmental research, vol 36. Nova Science Publishers Inc, New York, pp 217–234
5. Mukai SR (2012) Controlling the morphology of carbon gels. Boletin del Grupo Espanol del Carbon 26:8–11
6. Al-Muhtaseb SA, Ritter JA (2003) Preparation and properties of resorcinol-formaldehyde organic and carbon gels. Adv Mater 15(2):101–114
7. Lin-Zhi L, Shu-Hui T, Zaini MAA (2017) Carbon gel-based adsorbents for anionic dyes removal. In: Soon-Min H (ed) Activated carbon: prepared from various precursors. Ideal International E-Publication Pvt. Ltd., Indore, pp 62–84
8. Shu-Hui T, Zaini MAA (2017) Congo red removal by HNO_3-modified resorcinol-formaldehyde carbon gels. Chem Eng Trans 56:835–840
9. Lin-Zhi L, Zaini MAA (2017) Equilibrium and kinetic adsorption studies of reactive orange onto resorcinol-formaldehyde carbon gel. Chem Eng Trans 56:811–816
10. Zaini MAA, Yoshida S, Mori T, Mukai SR (2017) Preliminary evaluation of resorcinol-formaldehyde carbon gels for water pollutants removal. Acta Chimica Slovaca 10(1):54–60
11. Lagergren S (1898) About the theory of so-called adsorption of soluble substances (Kungliga svenska vetenskapsakademiens). Handlingar 24:1–39
12. Ho YS, McKay G (1998) A comparison of chemisorption kinetic models applied to pollutant removal on various sorbents. Process Saf Environ 76:332–340
13. Yoon YH, Nelson JH (1984) Application of gas adsorption kinetics: a theoretical model for respiratory cartridge service life. Am Ind Hyg Assoc J 45:509–516
14. Bohart GS, Adams EQ (1920) Some aspects of the behavior of charcoal with respect to chlorine. J Am Chem Soc 42:523–544
15. Thomas HC (1944) Heterogeneous ion exchange in a flowing system. J Am Chem Soc 66:1664–1666
16. Moreno-Castilla C, Maldonado-Hódar FJ (2005) Carbon aerogels for catalysis applications: an overview. Carbon 43:455–465
17. El-Khatat AM, Al-Muhtaseb SA (2011) Advances in tailoring resorcinol-formaldehyde organic and carbon gels. Adv Mater 23:2887–2903
18. Feng J, Feng J, Zhang C (2011) Shrinkage and pore structure in preparation of carbon aerogels. J Sol-Gel Sci Technol 59:371–380
19. Lima EC, Adebayo MA, Machado FM (2015) Chapter 3—Kinetic and equilibrium models of adsorption. In: Bergmann CP, Machado

FM (eds) Carbon Nanomaterials as adsorbents for environmental and biological applications. Springer, Berlin, pp 33–69
20. Zaini MAA, Meng TW, Kamaruddin MJ, Setapar SHM, Yunus MAC (2014) Microwave-induced zinc chloride activated palm kernel shell for dye removal. Sains Malaysiana 43(9):1421–1428
21. Alexander JA, Surajudeen A, Aliyu ENU, Omeiza AU, Zaini MAA (2017) Multi metals column adsorption of lead(II), cadmium(II) and manganese(II) onto natural bentonite clay. Water Sci Technol 76(8):2232–2241
22. Ahmad AA, Hameed BH (2010) Fixed-bed adsorption of reactive azo dye onto granular activated carbon prepared from waste. J Hazard Mater 175:298–303
23. Biswas S, Mishra U (2015) Continuous fixed-bed column study and adsorption modeling: removal of lead ion from aqueous solution by charcoal originated from chemical carbonization of rubber wood sawdust. J Chemistry. https://doi.org/10.1155/2015/907379